

See discussions, stats, and author profiles for this publication at: <https://www.researchgate.net/publication/263016323>

# Size and Phase Control of Cubic Lyotropic Liquid Crystal Nanoparticles

ARTICLE *in* THE JOURNAL OF PHYSICAL CHEMISTRY B · JUNE 2014

Impact Factor: 3.3 · DOI: 10.1021/jp502898a · Source: PubMed

---

CITATIONS

6

---

READS

29

## 5 AUTHORS, INCLUDING:



Katharina Ladewig (neé Porazik)

University of Melbourne

34 PUBLICATIONS 511 CITATIONS

[SEE PROFILE](#)



Andrea Janet O'Connor

University of Melbourne

76 PUBLICATIONS 1,372 CITATIONS

[SEE PROFILE](#)

# Size and Phase Control of Cubic Lyotropic Liquid Crystal Nanoparticles

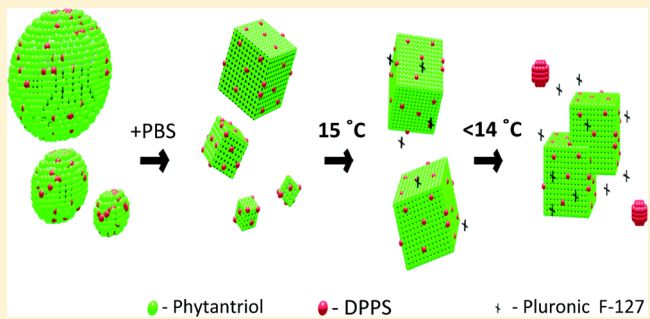
Terence E. Hartnett,<sup>†,‡</sup> Katharina Ladewig,<sup>†</sup> Andrea J. O'Connor,<sup>†</sup> Patrick G. Hartley,<sup>‡</sup> and Keith M. McLean<sup>\*,†</sup>

<sup>†</sup>Department of Chemical and Biomolecular Engineering and Particulate Fluids Processing Centre (PFPC), The University of Melbourne, Parkville, VIC 3010, Australia

<sup>‡</sup>Commonwealth Scientific and Industrial Research Organisation (CSIRO), Materials Science and Engineering, Clayton, VIC 3168, Australia

## Supporting Information

**ABSTRACT:** The effective use of lyotropic liquid crystalline dispersions, such as cubosomes, as drug delivery vehicles requires that they have tailored physical characteristics that suit specific therapeutics and external conditions. Here, we have developed phytantriol-based cubosomes from a dispersion of unilamellar vesicles and show that we can control their size as well as the critical packing parameter (CPP) of the amphiphilic bilayer through regulation of temperature and salt concentration, respectively. Using the anionic biological lipid 1,2-dipalmi-toylphosphatidylserine (DPPS) to prevent the cubic phase from forming, we show that the addition of phosphate buffered saline (PBS) results in a transition from small unilamellar vesicles to the cubic phase due to charge-shielding of the anionic lipid. Using dynamic light scattering, we show that the cubosomes formed following the addition of PBS are as small as 30 nm; however, we can increase the average size of the cubosomes to create an almost monodisperse dispersion of cubosomes through cooling. We propose that this phenomenon is brought about through the phase separation of the Pluronic F-127 used to stabilize the cubosomes. To complement previous work using the salt-induced method of cubosome production, we show, using synchrotron small-angle X-ray scattering (SAXS), that we can control the CPP of the amphiphile bilayer which grants us phase and lattice parameter control of the cubosomes.



## 1. INTRODUCTION

The development of drug delivery vehicles that can encapsulate, protect, and prolong the therapeutic effect of biomacromolecular therapeutics will increase patient comfort and bring substantial benefits to consumers. Recently, nanoparticle dispersions of the cubic phase of lyotropic liquid crystals (LLCs) have received increased attention for the purpose of drug delivery due to their potential to protect therapeutics from degradation and subsequently release them over a sustained time period.<sup>1–7</sup>

LLCs are formed through the self-assembly of a specific group of amphiphiles, such as phytantriol and glycerol monooleate (GMO) (Figure 1). Depending on their environment, these two amphiphiles may be present in various LLC phases including the lamellar, reverse micellar, hexagonal, and cubic phases (Figure 2). For example, when fully hydrated (>20% (w/v) water) and at room temperature, these two amphiphiles are present in the cubic phase. The nature of the cubic phase is such that it displays a specialized internal architecture resulting from the formation of a bicontinuous structure that creates an internal surface area of approximately 400 m<sup>2</sup>/g of amphiphile.<sup>8</sup> The specialized interwoven three-dimensional structure is attributable to the curvature of the

amphiphile bilayer, which generally forms around two non-intersecting water networks that traverse through the cubic phase, although interconnection in certain cases has recently been demonstrated.<sup>9</sup> The bicontinuous nature and high internal surface area are key factors that may make them amenable to sustained drug delivery.<sup>10–12</sup>

One limitation to the use of cubosomes as drug delivery vehicles for biologically based therapeutics, such as proteins, is the energy intensive methods used to produce them.<sup>2</sup> Traditional methods of cubosome production use sonication and homogenization to produce nanoparticles within a narrow size range.<sup>13,14</sup> Both methods are likely to denature biological molecules, such as proteins, rendering them inactive. Further, it has been suggested that cubosomes produced via these energy intensive methods are less stable, which—in a commercial sense—is not desirable.<sup>15</sup> Recently, new methods of cubosome production have been developed that may help to overcome these problems.<sup>4,15–17</sup> Muir et al. were able to show that cubosomes can be formed by the addition of phosphate

Received: March 24, 2014

Revised: May 26, 2014

Published: June 10, 2014

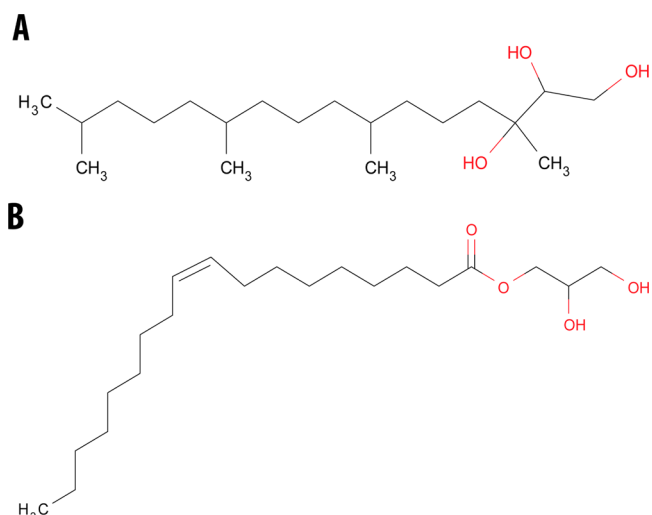


**Figure 1.** Chemical structures of the two common cubic phase forming amphiphiles (A) phytantriol and (B) glycerol monooleate (GMO).

buffered saline (PBS) to phytantriol-based small unilamellar vesicles (SUVs) that contained a charged lipid—dodecyldimethylammonium bromide (DDAB) (Figure 3A).<sup>17</sup> The presence of a charged lipid in the dispersion disrupts the cubic phase commonly found in phytantriol-based dispersions and produces SUVs instead of cubosomes on sonication. The addition of PBS then produces a charge-shield on the lipid, which subsequently alters the bilayer curvature and leads to the restoration of the cubic phase. Therefore, although energy intensive methods are still used to form a dispersion of vesicles, the final cubosome dispersion is formed through the simple addition of PBS. This investigation was recently followed up by Liu et al., who—using the anionic and cationic surfactants, sodium bis(2-ethylhexyl) sulfosuccinate (AOT) and DDAB, respectively—showed that the lattice parameter and phase of cubosomes produced through this method can be tailored by a similar mechanism to previously reported cosurfactant systems,<sup>6,7,18–24</sup> by modifying the concentration of the ionic lipid or salt in the dispersion.<sup>25</sup>

Using this “salt-induced” method of cubosome production, both Muir et al.<sup>17</sup> and Liu et al.<sup>25</sup> produced cubosomes that are similar in size to those prepared by traditional methods. However, the polydispersities of the resulting dispersions are significantly different, suggesting other environmental factors

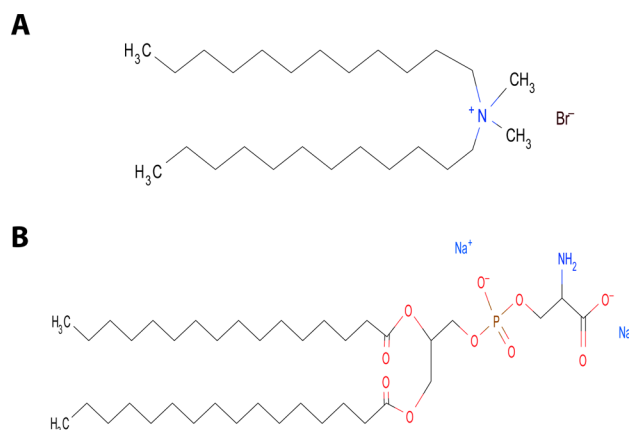


**Figure 3.** Chemical structures of the charged lipids (A) dodecyldimethylammonium bromide (DDAB) and (B) 1,2-dipalmitoylphosphatidylserine (DPPS).

may be influencing the size and polydispersity of the cubosomes. In addition, it has been demonstrated previously that the size of drug delivery vehicles plays a crucial role in their retention at the site of application.<sup>26–28</sup> Therefore, controlling both the size and polydispersity of cubosomes will maximize the potential of success for the delivery of therapeutics in the future.<sup>27</sup>

1,2-Dipalmitoylphosphatidylserine (DPPS) (Figure 3B) is an anionic lipid found in the inner leaflet of healthy mammalian cell membranes,<sup>29</sup> which makes it an excellent candidate lipid with which to fashion negatively charged cubosomes for the purposes of drug delivery. It has previously been shown that its addition to phytantriol-based dispersions leads to the disruption of the regular cubic phase and the formation of SUVs.<sup>30</sup> In a follow-up study, using a model cell membrane, it was shown that the introduction of a small amount of DPPS (2.5 wt %) into phytantriol cubosomes increases the interaction of the resulting cubosomes with the lipid bilayer membrane of mammalian cells.<sup>14</sup> This is important for the field of drug delivery, as it may enhance the intracellular delivery of therapeutics that are encapsulated within cubosomes.

Here, we investigate the role of different additives and environmental conditions on determining mesophase architecture and cubosome particle size. We first show that the addition of DPPS to phytantriol at concentrations above 8 wt % prevents the cubic phase from forming, resulting in the formation of SUVs only. In agreement with previous studies, we

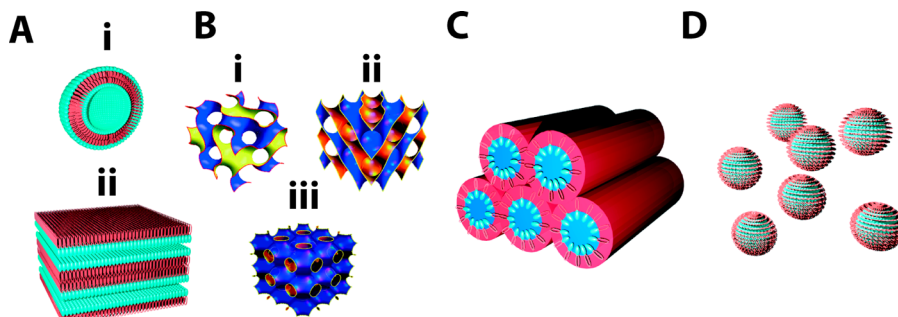


**Figure 2.** Structure of four different lyotropic liquid crystalline mesophases. (A) (i) A small unilamellar vesicle and (ii) the bulk lamellar phase. (B) The three inverse bicontinuous cubic subphases: (i) the gyroid ( $Ia\bar{3}d$ ) cubic phase, (ii) the diamond ( $Pn\bar{3}m$ ) cubic phase, and (iii) the primitive ( $Im\bar{3}m$ ) cubic phase. (C) The hexagonal phase and (D) the inverse micellar phase. Phytantriol and GMO may exist in any of these states depending on their environmental conditions.

find that the cubic phase can be restored by the addition of phosphate buffered saline (PBS). However, we demonstrate that the size of the cubosomes formed is much smaller than those produced through traditional methods of cubosome production. Secondly, we demonstrate that both size and phase of DPPSPhy cubosomes can be controlled via the regulation of temperature and ionic strength of the salt solution.

## 2. MATERIALS AND METHODS

**2.1. Materials.** Phytantriol (98%) was obtained from DSM Nutritional Products (Kaiseraugst, Switzerland), 1,2-dipalmitoyl-sn-glycero-3-phospho-L-serine, sodium salt (DPPS, Na) was obtained from Corden Pharmaceuticals (Liestal, Switzerland), and Pluronic F-127 (100:65:100) (poly(ethylene oxide)-poly(propylene oxide)-poly(ethylene oxide) and phosphate buffered saline tablets were purchased from Sigma-Aldrich (MO, USA). All materials were used as received.

**2.2. Preparation of Dispersions.** The phytantriol (Phy) and DPPS–phytantriol (DPPSPhy) mixtures were prepared by first dissolving phytantriol, F-127 (10 wt %), and DPPS in chloroform. The chloroform was removed by placing the sample in a rotary evaporator for 2 h and then in a desiccator overnight to ensure all of the chloroform was removed.

Prior to dispersion, the mixtures were heated until they were viscous and homogeneous. Water was added so that the concentration of phytantriol was 5% (w/v), and the mixture was dispersed by ultrasonication using a MisonixXL2000 (Misonix Inc., NY, USA) for 10 min (5 s on, 5 s off) at an amplitude of 70% of maximum output. The resulting SUV dispersions were allowed to stabilize at room temperature for at least 48 h prior to analysis.

Before analysis, either Milli-Q (Millipore, MA, USA) water or phosphate buffered saline (PBS) was added to the dispersions at a ratio of 2:1 (2 parts Milli-Q/PBS:1 part DPPSPhy dispersion). Temperature control of the dispersions was achieved by using a Thermomixer Comfort (Eppendorf, Hamburg, Germany).

**2.3. Particle Size.** Size and polydispersity of the dispersions were characterized by dynamic light scattering (DLS) using a Malvern Zeta-sizer 3000 (Malvern Instruments, Malvern, U.K.). Prior to analysis, samples were diluted with either PBS or H<sub>2</sub>O (1 μL:200 μL) to minimize interference from high turbidity. Samples prepared at low temperatures were tested at room temperature immediately following removal from the Thermo-mixer Comfort (Eppendorf, Hamburg, Germany). The samples were prepared in standard plastic disposable cuvettes.

**2.4. Cryo-TEM.** A laboratory-built humidity-controlled vitrification system was used to prepare the samples for Cryo-TEM. Humidity was kept close to 80% for all experiments, and ambient temperature was 22 °C. 200-mesh copper grids coated with perforated carbon film (Lacey carbon film: ProSciTech) were glow discharged in nitrogen prior to application of the sample. Subsequently, 4 μL aliquots of the sample were pipetted onto each grid. After 30 s of adsorption time, the grid was blotted manually using Whatman 541 filter paper, for approximately 2 s. Blotting time was optimized for each sample. Grids were then plunged into liquid ethane. Frozen grids were stored in liquid nitrogen until required.

The samples were examined using a Gatan 626 cryoholder (Gatan, CA, USA) and a Tecnai 12 Transmission Electron Microscope (FEI, Eindhoven, The Netherlands) at an operating voltage of 120 kV, with a Mega-view III CCD camera and AnalySIS camera control software (Olympus,

Tokyo, Japan). At all times, low dose procedures were followed, using an electron dose of 8–10 electrons/Å<sup>-2</sup> for all imaging. Images were recorded using magnifications in the range 30000× to 97000×.

**2.5. Small-angle X-ray scattering (SAXS).** SAXS experiments were performed on the SAXS/WAXS beamline at the Australian Synchrotron. In preparation, 80 μL portions of the samples were transferred into individual wells of a 96-well cell culture plate (CLS3695, Corning, NY, USA) and subsequently maintained at 25 °C until use. Samples were exposed to the 12 keV X-ray beam of dimensions 2500 μm × 130 μm and a typical flux of 5 × 10<sup>12</sup> photons/s, and diffraction patterns were recorded using a Pilatus 1 M detector (Dectris, Switzerland). A silver behenate standard was used to calibrate the reciprocal space vector for analysis. Data reduction (calibration and integration) was performed using AXcess, a custom-written SAXS analysis program written by Dr. Andrew Heron from Imperial College, London.<sup>31</sup>

## 3. RESULTS AND DISCUSSION

**3.1. Incorporation of DPPS into Phytantriol Dispersions—Cubic Phase Disruption.** The effect of DPPS incorporation into phytantriol dispersions was studied by varying the concentration of DPPS (0–16 wt %) included during the cubosome production. Dynamic light scattering (DLS) was then used to obtain the size and polydispersity of the nanoparticles followed by synchrotron small-angle X-ray scattering (SAXS) and cryogenic transmission electron microscopy (cryo-TEM) to assess the phase of the dispersions (Figure 4).

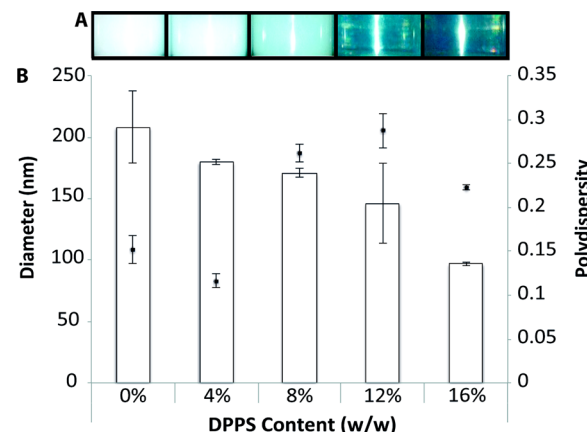


**Figure 4.** Influence of 1,2-dipalmitoylphosphatidylserine (DPPS) on phytantriol (Phy)-based dispersions (DPPSPhy/Phy). (A) Visual observations of phytantriol-based dispersions with increasing concentration range of DPPS. As the concentration of DPPS increases, the dispersions become translucent and then transparent when the concentration is ≥12 wt %. (B) Dynamic light scattering results for phytantriol dispersions containing increasing concentrations of DPPS. As the concentration increases, the size (bars) of the nanoparticles decreases and the polydispersity (points) increases.

The effect of the incorporation and increasing concentration of DPPS was a reduction in the optical density (Figure 4A). Pure phytantriol dispersions are “milky” in appearance, which is commonly attributed to the cubic phase,<sup>13,17</sup> while DPPSPhy dispersions with increasing amounts of DPPS become increasingly translucent until they become entirely transparent (>8 wt %). This value is comparable to the concentration of

DDAB and AOT required to prevent the cubic phase from forming as described by Liu et al.,<sup>25</sup> when using the same method of calculation.

DLS analysis of the obtained dispersions demonstrates that the largest nanoparticles are formed when only phytantriol is present in the dispersion, and as we increase the concentration of DPPS, the size of the nanoparticles decreases (Figure 4B).

By inserting itself into the phytantriol bilayer, the DPPS lipid reduces the negative curvature of the phytantriol bilayer which results in the appearance of a bilayer vesicle phase or, at high concentrations of DPPS, SUVs instead of cubosomes. The change in bilayer curvature is commonly attributed to a change of the critical packing parameter (CPP) of the amphiphile bilayer.<sup>32</sup> The CPP of the amphiphiles in the bilayer explains that a lamellar phase is observed when the CPP of the bilayer is between 0.5 and 1, while the cubic, hexagonal, and micellar cubic phases are observed when CPP > 1.<sup>33</sup> Hence, the large headgroup of DPPS must decrease the CPP of the amphiphilic bilayer from >1 to between 0.5 and 1.

Synchrotron SAXS confirms that the change observed in Figure 4A is due to the gradual disruption of the cubic phase as the DPPS content increases (Figure 5A). Bragg peaks indicative

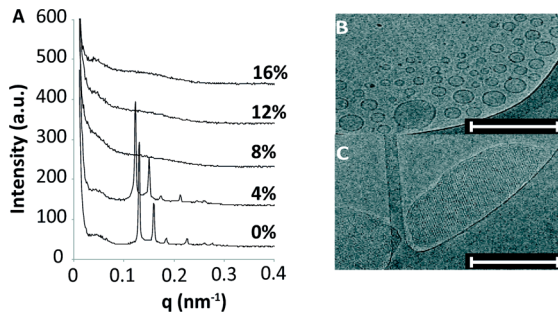


**Figure 5.** Synchrotron SAXS scatterplot (A) and cryo-TEM (B and C) of phytantriol (Phy)-based dispersions with increasing concentrations of DPPS. (A) Phy dispersions display Bragg peaks in the diamond ( $Pn3m$ ) phase, and as the concentration of DPPS increases, the Bragg peaks disappear from the scatterplot. This corresponds to a disruption of the cubic phase architecture. (B and C) Cryo-TEM of a Phy dispersion (bottom) and a DPPSPhy dispersion containing 12 wt % DPPS (top). Scale bar = 200 nm. Cryo-TEM confirms that the transparent dispersion that displayed no Bragg peaks in the scatterplot contains SUVs only.

of the  $Pn3m$  cubic phase are clearly observed for dispersions containing 0 and 4 wt % DPPS. These peaks move to the left as the concentration of DPPS increases, which results from the swelling of the cubic phase nanostructure, thus a shift toward a lower CPP. Although the dispersions containing 8 wt % DPPS exhibit no Bragg peaks in the SAXS scatterplot, it has been shown previously using cryo-TEM that these dispersions are biphasic in nature and experience both cubic phase and bilayer vesicle phase architecture.<sup>30</sup> Due to the increase in DPPS concentration and the absence of Bragg scattering produced from the samples containing 12 and 16 wt % DPPS, we believed these samples to contain SUVs only. The complete disruption of the cubic phase architecture is supported by cryo-TEM analysis (Figure 5B and C). The images support the DLS and SAXS data and demonstrate that the dispersion containing 12 wt % DPPS (Figure 5B) is composed of SUVs, while the phytantriol-only dispersion (Figure 5C) is composed of large cubosomes.

**3.2. Salt-Induced Charge-Shielding—Restoration of the Cubic Phase.** Charge-shielding experiments were performed with dispersions that contained DPPSPhy SUVs only (i.e., 12 and 16 wt % DPPS). Charge-shielding was induced in the DPPSPhy SUVs (12 and 16 wt % DPPS) by the addition of PBS in a volume ratio of 1:2, i.e., 50  $\mu\text{L}$  of dispersion + 100  $\mu\text{L}$  of PBS, to give a final salt concentration of 150 mM (1× PBS), the same ionic strength as found in physiological conditions,<sup>34</sup> or 1.5 M (10× PBS). Immediately following the addition of PBS, an increase in optical density was observed (Figure 6A); however, the dispersions were less

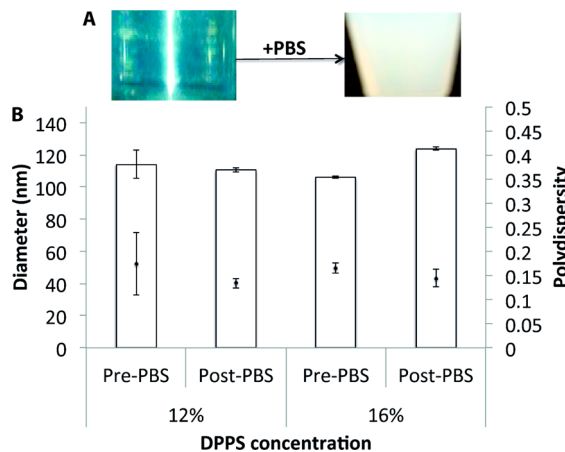


**Figure 6.** Visual (A) and size (B) characteristics of phytantriol dispersions containing DPPS (12 and 16 wt %).

“milky” than expected and appeared translucent instead, which is different from the results observed by both Muir et al. and Liu et al. using the ionic surfactants DDAB (Liu and Muir) and AOT (Liu).<sup>17,25</sup> Similarly, DLS analysis of the dispersions prior to and after the addition of PBS shows no noteworthy change in the size or polydispersity of the dispersions (Figure 6B).

Visual and DLS indicate that only a restricted phase transition from SUVs to a cubic-bilayer vesicle phase may be occurring. To further examine the phase transitions that occurred in the dispersions before and after the addition of PBS, we used synchrotron SAXS (Figure 7). Although only very low intensity Bragg peaks are observed in the scatterplots, SAXS confirmed that addition of PBS to DPPSPhy SUVs does indeed lead to the formation of cubosomes. These cubosomes appear to be in the  $Pn3m$  cubic phase; however, as the scattering intensity is low and there are only two peaks visible, it is difficult to confirm the exact phase of the cubosomes in the dispersions, unlike the phytantriol-only sample.

The presence of low intensity or the absence of peaks following the addition of PBS may be a byproduct of the previously discussed restricted phase transition from SUVs to a cubic-bilayer vesicle phase, since any bilayer vesicle phase present would not contribute to the scattering pattern in Figure 7. To investigate why the Bragg peak intensity did not match that of the previously reported data, we employed cryo-TEM to visualize the dispersion. Cryo-TEM confirmed that the addition of PBS to the DPPSPhy SUVs did result in the desired cubic phase transition (Figure 8). We observed that the cubosomes produced using the PBS method are much smaller than those produced using traditional methods and believe that this may be the cause of the low intensity Bragg peaks observed in the SAXS scatterplot when compared to the phytantriol-only

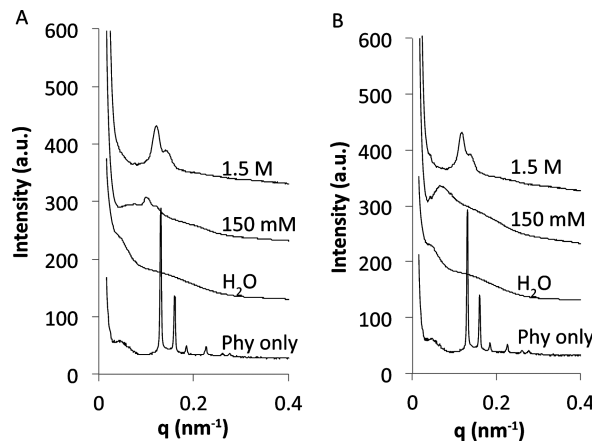


**Figure 7.** Scatterplots obtained through small angled X-ray scattering (SAXS) of phytantriol dispersions containing 12 wt % (A) and 16 wt % (B) DPPS in  $\text{H}_2\text{O}$ , 150 mM salt and 1.5 M salt. The scatter profile of a phytantriol-only dispersion is included at the bottom of the plot as a reference only. (A) When in water, the 12 wt % sample displays no Bragg peaks. The addition of a salt solution leads to the formation of low intensity Bragg peaks for both the 150 mM and 1.5 M samples. (B) When in water or in a 150 mM salt solution, the 16 wt % sample displays no discernible Bragg peaks. The addition of a high concentration salt solution, 1.5 M, leads to the formation of Bragg peaks in both the 12 and 16 wt % DPPS samples; however, exact phase recognition is difficult due to the presence of only two Bragg peaks.

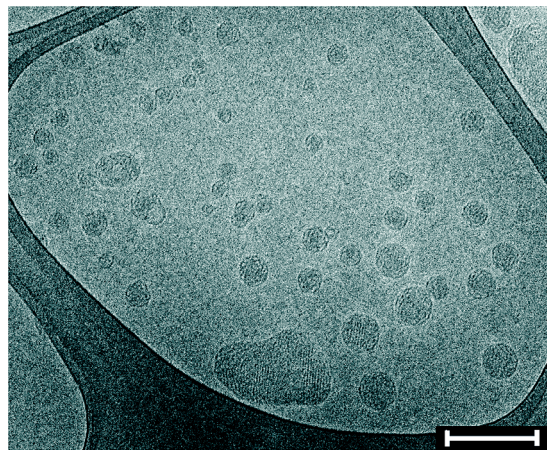


**Figure 8.** Cryo-TEM image obtained of a DPPSPhy dispersion prepared and kept at 20 °C. The cubic phase nanoparticles are very small and have a high polydispersity, which corresponds to the data obtained through dynamic light scattering. Scale bar = 200 nm.

sample. The particle sizes and polydispersity observed using cryo-TEM are in agreement with the DLS data.

Interestingly, the phase transition that is occurring requires that the SUVs, hollow spheres of amphiphiles, be converted to cubosomes, which are densely packed amphiphilic nanoparticles. The size data, however, shows that the average size of the nanoparticles in the dispersion before and after the addition of PBS remains stable or even increases. This indicates that there is some form of renucleation or clustering of the newly formed cubosomes following the addition of PBS.

Clustering of lyotropic liquid crystalline phase nanoparticles has been reported previously.<sup>35–37</sup> Angelov et al. predicted the growth of the  $Pn3m$  cubic phase,<sup>36</sup> and have recently demonstrated this experimentally from a curved lipid bilayer.<sup>37</sup> They found that the transition from SUVs to the cubic phase

has an intermediate tetrahedral packed bilayer vesicle stage before forming the larger cubosomes. These unstable lipid membrane structures require growth to occur in order to reach a stable  $Pn3m$  configuration. We believe that this, or something similar, is occurring in the DPPSPhy transition.

We can conclude that salt-induced charge-shielding of the DPPSPhy SUVs by means of PBS addition restores the cubic phase. Charge-shielding of the DPPS lipid reduces the size of its hydrophilic headgroup, thereby restoring the curvature of the phytantriol bilayer and the cubic structure. Successful incorporation of DPPS within the bilayer is evident by the shift of the primary Bragg peak in the SAXS scatterplot to a lower  $q$ -value than the phytantriol-only sample (Figure 7).

**3.3. Salt-Induced Charge-Shielding—Effect of Temperature on LLC Nanoparticle Size and Phase.** The discrepancies observed between the polydispersity in the different studies suggest that the size of the cubosomes produced through the salt-induced method is influenced by factors other than just the addition of PBS to the dispersion containing SUVs. It has previously been proposed that cooling of anionic lipids like those found in cellular membranes can lead to cubic phase transitions and that this may be due to the phase separation of the lipid or due to an increase in charge-shielding as the temperature approaches freezing.<sup>38</sup> We therefore, studied the effect of temperature on DPPSPhy cubosomes, which were produced using the salt-induced charge-shielding method, by cooling the dispersions immediately after the addition of PBS. The dispersions were then allowed to return to room temperature before being analyzed by DLS, cryo-TEM, and synchrotron SAXS (Figure 9).

The first observation upon cooling of the dispersions from 20 to 15 °C was the re-emergence of the “milky” appearance (Figure 9A) that was lacking in the previous experiments, all of which were conducted at room temperature. We attribute this to the presence of larger and hence better scattering particles within the dispersion. This was confirmed by DLS analysis (Figure 9B), where decreasing the temperature led to an increase particle size and a drop in polydispersity. This trend is, however, reversed once the temperature is reduced below 15 °C with both larger particle sizes and polydispersity being observed as the temperature was decreased further. It is likely that an Ostwald ripening phenomenon, whereby the larger cubosomes grow at the expense of the smaller ones, may explain the observed changes of size and polydispersity.<sup>39</sup> When the temperature is first reduced, the smaller cubosomes are incorporated into the larger cubosomes. The loss of the smaller cubosomes from the dispersion leads to the observed increase in average size and reduction in polydispersity. However, once the smaller cubosomes are consumed, the larger cubosomes begin to coalesce, which leads to the significant size and polydispersity increases observed when the temperature reaches 12 °C. LLC nanoparticle growth similar to this has previously been reported in glycerol monooleate-based dispersions.<sup>3,13</sup>

Since different regions of the body have specific size requirements for drug delivery vehicles to be successful, the ability to control the size and polydispersity of the cubosomes by regulating the temperature is important for their potential use as drug delivery vehicles. For instance, the eye, a complicated region of multiple tissues and barriers, has different requirements for a vehicle depending on the region to be targeted. An injectable delivery vehicle for use under the conjunctival layer of the eye requires that the size of the vehicle must be tailored to suit the specific applications of the

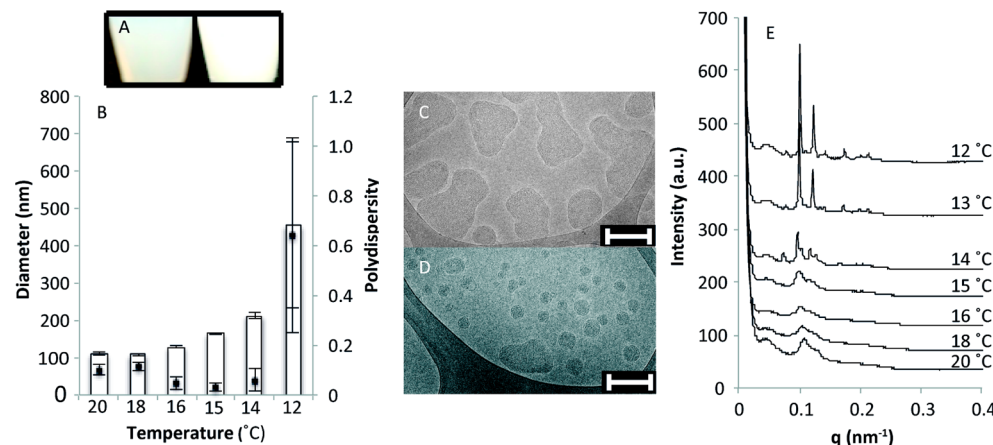


**Figure 9.** Influence of temperature on phytantriol-based dispersions containing 12 wt % dipalmitoylphosphatidyl serine (DPPSPhy). (A) DPPSPhy dispersions kept at 20 °C (left) and after being cooled 15 °C (right). (B) Dynamic light scattering (DLS) of DPPSPhy dispersions that have been cooled. As the temperature is reduced to 15 °C, the size of the nanoparticles (bars) increases and the polydispersity (points) decreases. (C and D) Cryo-TEM images of a DPPSPhy dispersion that was cooled to 15 °C (D) and a dispersion that was kept at room temperature following the addition of PBS. Scale bar = 200 nm. (E) Scatterplot obtained through small angled X-ray scattering (SAXS) of DPPSPhy dispersions that have been cooled from 20 to 12 °C. All profiles were obtained at room temperature.

therapeutic. Amrite et al. have shown that small nanoparticles (20 nm) are removed from the site of treatment and it may be expected that some, if not most, will end up in the ocular circulatory system. On the other hand, in the same study, larger particles (200 nm) were found to remain at the site of administration following injection, thus providing sustained release of the therapeutic.<sup>28</sup>

In addition to the possible applications using cubosomes, the observed formation of coalesced/bulk cubic phase following cooling to lower temperatures may be an important step for the use of cubic-phase-based gels for the topical delivery of bioactive therapeutic drugs. Assuming that the bulk phase that forms following cooling of the dispersion has the same internal characteristics as the nanoparticle dispersions, cooling would provide an easy route to encapsulate bioactive therapeutics into the bulk cubic phase with the potential to act as a drug delivery depot formulation.

Synchrotron SAXS revealed that DPPSPhy cubosomes which are cooled from 20 to 14 °C experience an increase in lattice parameter, which is evident by the shift of the primary peak to the left (Figure 9E). This could be attributed to the commonly observed phenomenon that cooling of self-assembled lipid structures results in a reduction in bilayer curvature and thus an increase in lattice parameter.<sup>20</sup> However, this only applies if the dispersions are actually studied at a lower temperature and are not brought back to room temperature prior to characterization, as was the case in our experiments. Therefore, other underlying factors must contribute to the observed irreversible shift of lattice parameter in these samples. In addition to the observed increase in lattice parameter as the temperature is reduced from 20 to 14 °C, the overall peak intensity increases and additional peaks, attributed to the *Im3m* cubic phase, appear in these scatterplots. These irreversible changes indicate that a biphasic *Pn3m/Im3m* cubic system is formed when samples are incubated at lower temperatures. A continued reduction in temperature (<14 °C) leads to a further increase in peak intensity; however, the peaks now begin to shift to the right of the scatterplot, indicating a reduction of the lattice parameter within the cubosomes. (Figure 9E).

These discontinuous trends are perplexing at first sight, and a number of explanations might be considered. Charge-shielding

of lipid headgroups at lower temperatures, as postulated by Quinn et al.,<sup>38</sup> would be expected to cause an effective smaller headgroup and a shift toward the phytantriol bilayer architecture due to increased negative bilayer curvature. One would, however, expect this change to be completely reversible when temperature was increased, which is not observed here.

This leaves phase separation of one of the components of the DPPSPhy dispersions as an explanation for the observed size and phase differences between DPPSPhy cubosomes prepared at 20 °C and those prepared/incubated at lower temperatures. Of the three components in the system, phase separation of the phytantriol can be ruled out because if this were occurring one would expect to see a change in the Bragg peak patterning in the SAXS scatterplot, however, not the changes to the Bragg peak positioning we observed. If phytantriol were phase separating from the PhyDPPS cubosomes, then one would expect the influence of the DPPS in the dispersion to become greater, causing a shift in the Bragg peak position to the left of the scatterplot. In addition, one would expect a reduction in the Bragg peak intensity, as the concentration of cubic phase in the dispersion would reduce (i.e., the CPP of the bilayer shifts towards the lamellar phase), resulting in reduced scattering. Although we initially observed a shift of the Bragg peaks to the left of the scatterplot, this shift switches at 14 °C and the Bragg peaks then shift to the right of the scatterplot. In addition, we observed an increase in the Bragg peak intensity, not a reduction (Figure 5). This leaves phase separation of either DPPS or the Pluronic F-127 (F-127).

If the DPPS was expelled from the cubosomes during cooling, then the lattice parameter of the dispersion (obtained through SAXS) would be expected to decrease as the DPPS separates from the cubosome and the phase would shift toward that of the natural *Pn3m* phase of phytantriol. In the SAXS scatterplots in Figure 9, we see that below 14 °C there is a shift in the SAXS peak position to higher *q*-values (smaller lattice parameters). This change suggests that phase separation of DPPS may be occurring (with an increased tendency toward phytantriol architecture) when the DPPSPhy cubosomes are cooled to below 14 °C. However, phase separation of DPPS does not explain the changes that are occurring from 20 to 14 °C. In fact, within the temperature range from 20 to 14 °C,

we observe peak shifts to lower  $q$ -values, which suggests increasing water channel diameters within the cubic phase nanoparticles.

The stability of both the DPPSPhy and the phytantriol-only cubosomes stems from the presence of the F-127—without it, the nanoparticle dispersions are unstable, which leads to coalescence of the cubosomes and ultimately to the formation of the bulk cubic phase.<sup>40</sup>

F-127 is a block copolymer, which in itself has been proposed as a micellar drug delivery vehicle,<sup>41</sup> and which shows a concentration dependent temperature-response curve.<sup>42</sup> The critical micellization temperature (CMT), the temperature below which the surfactant forms micelles in aqueous solution, increases with a decreasing concentration of F-127. The CMT of F-127 at a concentration of 10 mg/mL is approximately 24 °C. Our DPPSPhy and phytantriol dispersions contain 6.4 mg/mL F-127, a concentration which points to a CMT that is higher than the 24 °C obtained in the F-127-only system. However, the presence of other amphiphiles such as DPPS and phytantriol as well as the presence of salts, such as NaCl, has been shown to influence the CMT of F-127;<sup>43</sup> hence, the temperature at which F-127 phase-separates from the cubosomes in the present system is significantly different to a system which contains F-127 dispersed in water alone.

Given the results shown in Figure 9, we suspect that the CMT of F-127 in our dispersion may be approximately 15 or 16 °C, as this is the point where we begin to see the “milky” appearance usually attributed to the cubic phase and the temperature that the average particle size begins to increase. Partial phase separation of the F-127 from the DPPSPhy system as the dispersions are cooled from 20 to 14 °C leads to an increase in average cubosome size (as individual nanoparticles experience less stabilization and coalesce) and, due to what we believe is a similar process to Ostwald ripening, a simultaneous decrease in polydispersity (Figure 10). Once the temperature falls below the CMT, the F-127 will begin to form micelles, resulting in aggregation of the cubosomes present in the dispersion.

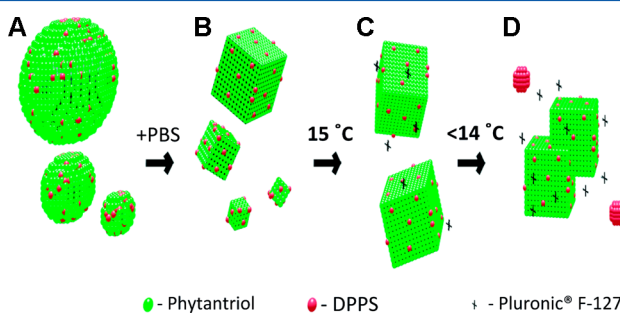


**Figure 10.** Schematic of the changes observed in DPPSPhy dispersions. (A) Following sonication of a mixture of DPPS (red) and phytantriol (green), small unilamellar vesicles (SUVs) form. (B) The addition of PBS leads to charge-shielding of the DPPS lipid which reduces the headgroup size of DPPS and allows the cubic phase to form. (C) When the temperature is reduced, the Pluronic F-127 (F-127), which is used to stabilize cubosomes, forms micelles, and this results in the smaller cubosomes aggregating to form larger ones. This increases the average size of the cubosome dispersion and decreases the polydispersity. (D) When the temperature is reduced below 14 °C, we observe phase separation of the F-127 and DPPS from the cubosomes.

We believe that phase separation of F-127 and the subsequent coalescence of the smaller nanoparticles also explains the appearance of Bragg peaks in the scatterplot that correspond to the  $Im\bar{3}m$  phase as the temperature is decreased from 20 to 14 °C. When the size and polydispersity of the dispersions were measured in water, we observed a relationship between the concentration of DPPS present within the dispersion and the size of the vesicles: as the concentration increased, the average diameter of the nanoparticles decreased (Figure 4B). When we then induced the cubic phase transition through the addition of PBS, we anticipated that these SUVs will form correspondingly small cubosomes with larger water channels due to the higher concentration of DPPS present within the bilayer. However, due to their size, these cubosomes were not detectable in the SAXS scatterplots for samples prepared above 14 °C. When we decrease the temperature, these smaller cubosomes, with a relatively higher concentration of DPPS, coalesce to form larger cubosomes with larger water channels which we correlate with the higher intensity peaks in the  $Im\bar{3}m$  phase in the SAXS scatterplot.

**3.4. Salt-Induced Charge-Shielding—Effect of Salt Concentration on LLC Nanoparticle Phase.** Phytantriol cubosomes are generally found in the  $Pn\bar{3}m$  cubic phase when in excess water and have a lattice parameter of close to 68 Å (Table S1, Supporting Information). A lattice parameter of this size provides a restricted environment and area in which to encapsulate hydrophilic therapeutics and may be insufficient for the encapsulation of some larger therapeutics such as some globular proteins. Modifying the environmental conditions of phytantriol can, however, result in changes in the phase and lattice parameter of cubosomes. Liu et al.<sup>25</sup> described the transition of the AOT and DDAB dispersions from SUVs to cubic phase nanoparticles to be dependent on the CPP of the amphiphile bilayer. As we have shown above, the addition of PBS to DPPSPhy SUVs results in the self-assembly of cubosomes that have a larger lattice parameter than phytantriol-only cubosomes. The difference between the phase and lattice parameter of phytantriol-only cubosomes and those of the salt-induced DPPSPhy cubosomes can also be attributed to the ability of DPPS and PBS to influence the critical packing parameter (CPP) of the DPPSPhy bilayer. We therefore hypothesized that—similarly to the behavior observed by Liu et al.<sup>25</sup>—by controlling the concentration of DPPS and PBS it should be possible to control the phase and lattice parameter of DPPSPhy cubosomes produced via the salt-induced method. In order to test this hypothesis, a series of DPPSPhy dispersions containing varying amounts of DPPS were prepared. Subsequently, water or PBS of varying concentration was added and the samples analyzed via synchrotron SAXS (Figure S1 and Table S1, Supporting Information).

The control that DPPS and PBS exert on the phase and lattice parameters of the cubosomes is in agreement with the observation made by Liu et al.<sup>25</sup> using the ionic surfactants AOT and DDAB. As discussed earlier, changes in the internal curvature of amphiphilic mesophases are dependent on the critical packing parameter (CPP) of the amphiphiles within the bilayer.<sup>44</sup> We find here that the limiting factor to changes in the CPP in DPPSPhy dispersions is the uncharged phytantriol. As phytantriol is naturally observed in the  $Pn\bar{3}m$  phase and is not influenced by the PBS concentration, we do not observe any further reductions in the CPP from that seen in the phytantriol-only sample.

By adjusting the concentration of PBS and DPPS, we can regulate the curvature of the bilayer by changing the CPP, which in turn grants us control over the lattice parameter and phase of the dispersions. We believe this will be an important step for the use of cubosomes in any application where regulating the diffusion of particles or therapeutics is important, as the size of the water channels will directly influence the maximum size of hydrophilic therapeutics that can be encapsulated within cubosomes. In addition to increasing the likelihood of successful encapsulation of larger therapeutics, controlling the water channel diameter is important for controlling the release kinetics of encapsulated therapeutics;<sup>6,45</sup> i.e., a small therapeutic migrating through a relatively large water channel will experience less hindered diffusion compared to a tailored water channel, which may control diffusion by restricting the therapeutic movement.

The combinatorial effect that PBS and DPPS have on the phase of phytantriol dispersions is summarized in Figure 11.

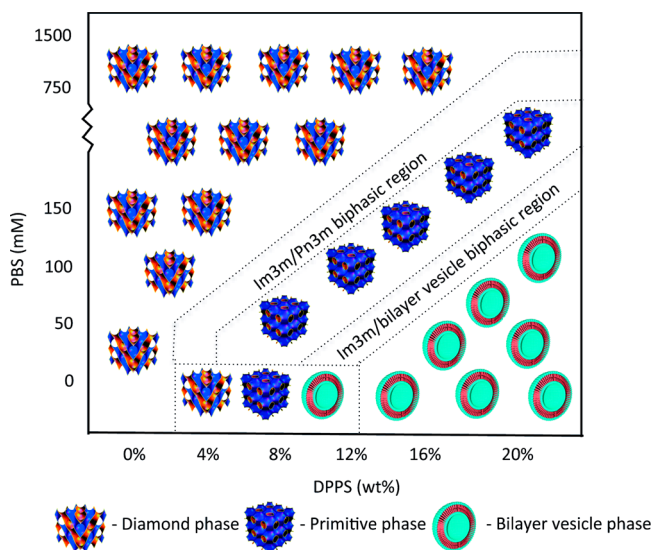


**Figure 11.** Phase diagram showing the contrasting effects of PBS and DPPS on the phase of phytantriol-based dispersions. DPPS reduces the critical packing parameter of the bilayer and causes the dispersions to form small unilamellar vesicles (SUVs) upon dispersion, while PBS acts to restore the packing parameter back to that of a phytantriol-only sample. The data points shown are representative of the phases observed following SAXS analysis of the phytantriol-based dispersions (Figure S1, Supporting Information).

This relationship is dependent on both the size and charge of the DPPS headgroup and is therefore not a general representation of the influence that ionic amphiphiles or other surfactants have on phytantriol dispersions, but rather it is specific to DPPS. This is supported by the different effects that cosurfactant have on the phase behavior of both GMO and phytantriol-based systems.<sup>6,7,17–23,25,37</sup> The role of each surfactant is to change the CPP of the amphiphilic bilayer which, if the changes can be reversed through environmental control, provides the ability to control the phase and lattice parameter of the cubosomes.

#### 4. CONCLUSION

In summary, we have shown that the incorporation of the anionic membrane lipid DPPS into phytantriol-based dispersions leads to a complete disruption of the usual cubic

structure of phytantriol nanoparticles, resulting in the formation of a vesicle phase once the DPPS content exceeds 8 wt %. However, the cubic phase can be readily restored via salt-induced charge-shielding, which results in negatively charged cubosomes in a size range suitable for a variety of drug delivery applications.

We further show that temperature can be used to modify the size and phase of these cubosomes and demonstrate that partial phase separation of the stabilizing agent Pluronic F-127 underpins these changes.

Lastly, we show that the phase and lattice parameters of cubosomes produced through the charge-shielding method can be readily tailored by controlling the amount of DPPS in the phytantriol-based dispersions as well as by controlling the concentration of PBS added to these dispersions. The control that PBS and DPPS exhibit on the lattice parameter of phytantriol-based dispersions therefore presents an opportunity to tailor cubosomes for the size specific encapsulation of therapeutics.

#### ■ ASSOCIATED CONTENT

##### ● Supporting Information

Lattice parameters and SAXS scatterplots of Phy and DPPSPhy dispersions at different PBS concentrations. This material is available free of charge via the Internet at <http://pubs.acs.org>.

#### ■ AUTHOR INFORMATION

##### Corresponding Author

\*E-mail: keith.mclean@csiro.au. Phone: +61 3 9545 2599.

##### Author Contributions

The manuscript was written through contributions of all authors. All authors have given approval to the final version of the manuscript.

##### Notes

The authors declare no competing financial interest.

#### ■ ACKNOWLEDGMENTS

T.E. Hartnett would like to thank The University of Melbourne, the Commonwealth Scientific and Industrial Research Organisation (CSIRO), and the Melbourne Materials Institute (MMI) for various scholarships. K. Ladewig acknowledges financial support from the Australian Research Council (ARC) in the form of an ARC Super Science Fellowship (FS 110200025). Infrastructure support from the Particulate Fluids Processing Centre (PFPC), the MMI, CSIRO and The University of Melbourne is gratefully acknowledged. This research was undertaken on the SAXS/WAXS beamline at the Australian Synchrotron, Victoria, Australia (MS720). Cryo-TEM images were obtained with the assistance of Ms. Lynne Waddington, CSIRO, Parkville. Financial support was also provided by the National Health and Medical Research Council (NHMRC, Program Grant 1047603).

#### ■ ABBREVIATIONS

PBS, phosphate buffered saline; CPP, critical packing parameter; DPPS, 1,2-dipalmitoylphosphatidylserine; LLC, lyotropic liquid crystal; GMO, glycerol monooleate; DDAB, dodecyldimethylammonium bromide; AOT, sodium bis(2-ethylhexyl) sulfosuccinate; DPPSPhy, 1,2-dipalmitoylphosphatidylserine/phytantriol; SAXS, small-angle X-ray scattering; DLS, dynamic light scattering; Cryo-TEM, cryogenic transmission electron microscopy

## ■ REFERENCES

- (1) Angius, R.; Murgia, S.; Berti, D.; Baglioni, P.; Monduzzi, M. Molecular Recognition and Controlled Release in Drug Delivery Systems Based on Nanostructured Lipid Surfactants. *J. Phys.: Condens. Matter* **2006**, *18*, S2203–S2220.
- (2) Mulet, X.; Boyd, B. J.; Drummond, C. J. Advances in Drug Delivery and Medical Imaging Using Colloidal Lyotropic Liquid Crystalline Dispersions. *J. Colloid Interface Sci.* **2013**, *393*, 1–20.
- (3) Angelov, B.; Angelova, A.; Papahadjopoulos-Sternberg, B.; Hoffmann, S. V.; Nicolas, V.; Lesieur, S. Protein-Containing PEGylated Cubosomes: Freeze-Fracture Electron Microscopy and Synchrotron Radiation Circular Dichroism Study. *J. Phys. Chem. B* **2012**, *116*, 7676–7686.
- (4) Angelov, B.; Angelova, A.; Filippov, S. K.; Karlsson, G.; Terrill, N.; Lesieur, S.; Štěpánek, P. Topology and Internal Structure of PEGylated Lipid Nanocarriers for Neuronal Transfection: Synchrotron Radiation SAXS and Cryo-TEM Studies. *Soft Matter* **2011**, *7*, 9714–9720.
- (5) Angelov, B.; Angelova, A.; Filippov, S. K.; Narayanan, T.; Drechsler, M.; Štěpánek, P.; Couvreur, P.; Lesieur, S. DNA/Fusogenic Lipid Nanocarrier Assembly: Millisecond Structural Dynamics. *J. Phys. Chem. Lett.* **2013**, *4*, 1959–1964.
- (6) Negrini, R.; Mezzenga, R. Diffusion, Molecular Separation, and Drug Delivery from Lipid Mesophases with Tunable Water Channels. *Langmuir* **2012**, *28*, 16455–16462.
- (7) Negrini, R.; Mezzenga, R. pH-Responsive Lyotropic Liquid Crystals for Controlled Drug Delivery. *Langmuir* **2011**, *27*, 5296–5303.
- (8) Lawrence, M. Surfactant Systems: Their Use in Drug Delivery. *Chem. Soc. Rev.* **1994**, *23*, 417–424.
- (9) Zabara, A.; Negrini, R.; Onaca-Fischer, O.; Mezzenga, R. Perforated Bicontinuous Cubic Phases with pH-Responsive Topological Channel Interconnectivity. *Small* **2013**, *9*, 3602–3609.
- (10) Yang, D.; O'Brien, D.; Marder, S. Polymerized Bicontinuous Cubic Nanoparticles (cubosomes) from a Reactive Monoacylglycerol. *J. Am. Chem. Soc.* **2002**, *124*, 13388–13389.
- (11) Angelova, A.; Angelov, B.; Garamus, V. M.; Couvreur, P.; Lesieur, S. Small-Angle X-Ray Scattering Investigations of Biomolecular Confinement, Loading, and Release from Liquid-Crystalline Nanochannel Assemblies. *J. Phys. Chem. Lett.* **2012**, *3*, 445–457.
- (12) Jeong, S.; O'Brien, D.; Orädd, G.; Lindblom, G. Encapsulation and Diffusion of Water-Soluble Dendrimers in a Bicontinuous Cubic Phase. *Langmuir* **2002**, *18*, 1073–1076.
- (13) Barauskas, J.; Johnsson, M.; Joabsson, F.; Tiberg, F. Cubic Phase Nanoparticles (Cubosome): Principles for Controlling Size, Structure, and Stability. *Langmuir* **2005**, *21*, 2569–2577.
- (14) Shen, H.-H.; Hartley, P. G.; James, M.; Nelson, A.; Defendi, H.; McLean, K. M. The Interaction of Cubosomes with Supported Phospholipid Bilayers Using Neutron Reflectometry and QCM-D. *Soft Matter* **2011**, *7*, 8041–8049.
- (15) Spicer, P.; Hayden, K.; Lynch, M.; Ofori-Boateng, A.; Burns, J. Novel Process for Producing Cubic Liquid Crystalline Nanoparticles (cubosomes). *Langmuir* **2001**, *17*, 5748–5756.
- (16) Awad, T. S.; Okamoto, Y.; Masum, S. M.; Yamazaki, M. Formation of Cubic Phases from Large Unilamellar Vesicles of Doleoylphosphatidylglycerol/monoolein Membranes Induced by Low Concentrations of Ca<sup>2+</sup>. *Langmuir* **2005**, *21*, 11556–11561.
- (17) Muir, B. W. B.; Zhen, G.; Gunatillake, P.; Hartley, P. G. Salt Induced Lamellar to Bicontinuous Cubic Phase Transitions in Cationic Nanoparticles. *J. Phys. Chem. B* **2012**, *116*, 3551–3556.
- (18) Zabara, A.; Mezzenga, R. Plenty of Room to Crystallize: Swollen Lipid Mesophases for Improved and Controlled in-Meso Protein Crystallization. *Soft Matter* **2012**, *8*, 6535–6541.
- (19) Zabara, A.; Mezzenga, R. Modulating the Crystal Size and Morphology of in Meso-Crystallized Lysozyme by Precisely Controlling the Water Channel Size of the Hosting Mesophase. *Soft Matter* **2013**, *9*, 1010–1014.
- (20) Angelov, B.; Angelova, A.; Ollivon, M.; Bourgaux, C.; Campitelli, A. Diamond-Type Lipid Cubic Phase with Large Water Channels. *J. Am. Chem. Soc.* **2003**, *125*, 7188–7189.
- (21) Yaghmur, A.; Laggner, P.; Zhang, S.; Rappolt, M. Tuning Curvature and Stability of Monoolein Bilayers by Designer Lipid-like Peptide Surfactants. *PLoS One* **2007**, *2*, e479.
- (22) Yaghmur, A.; de Campo, L.; Sagalowicz, L.; Leser, M. E.; Glatter, O. Control of the Internal Structure of MLO-Based Isosomes by the Addition of Diglycerol Monooleate and Soybean Phosphatidylcholine. *Langmuir* **2006**, *22*, 9919–9927.
- (23) Angelova, A.; Angelov, B.; Lesieur, S.; Mutafchieva, R.; Ollivon, M.; Bourgaux, C.; Willumeit, R.; Couvreur, P. Dynamic Control of Nanofluidic Channels in Protein Drug Delivery Vehicles. *J. Drug Delivery Sci. Technol.* **2008**, *18*, 41–45.
- (24) Angelova, A.; Ollivon, M.; Campitelli, A.; Bourgaux, C. Lipid Cubic Phases as Stable Nanochannel Network Structures for Protein Biochip Development: X-Ray Diffraction Study. *Langmuir* **2003**, *19*, 6928–6935.
- (25) Liu, Q.; Dong, Y.-D.; Hanley, T. L.; Boyd, B. J. Sensitivity of Nanostructure in Charged Cubosomes to Phase Changes Triggered by Ionic Species in Solution. *Langmuir* **2013**, *29*, 14265–14273.
- (26) Sahoo, S. K.; Dilnawaz, F.; Krishnakumar, S. Nanotechnology in Ocular Drug Delivery. *Drug Discovery Today* **2008**, *13*, 144–151.
- (27) Vonarbourg, A.; Passirani, C.; Saulnier, P.; Benoit, J.-P. Parameters Influencing the Stealthiness of Colloidal Drug Delivery Systems. *Biomaterials* **2006**, *27*, 4356–4373.
- (28) Amrite, A. C.; Komppella, U. B. Size-Dependent Disposition of Nanoparticles and Microparticles Following Subconjunctival Administration. *J. Pharm. Pharmacol.* **2005**, *57*, 1555–1563.
- (29) Fadok, V. a.; Voelker, D. R.; Campbell, P. a.; Cohen, J. J.; Bratton, D. L.; Henson, P. M. Exposure of Phosphatidylserine on the Surface of Apoptotic Lymphocytes Triggers Specific Recognition and Removal by Macrophages. *J. Immunol.* **1992**, *148*, 2207–2216.
- (30) Shen, H.; Crowston, J.; Huber, F.; Saubern, S.; Mclean, K. M.; Hartley, P. G. The Influence of Dipalmitoyl Phosphatidylserine on Phase Behaviour of and Cellular Response to Lyotropic Liquid Crystalline Dispersions. *Biomaterials* **2010**, *31*, 9473–9481.
- (31) Seddon, J. M.; Squires, A. M.; Conn, C. E.; Ces, O.; Heron, A. J.; Mulet, X.; Shearman, G. C.; Templer, R. H. Pressure-Jump X-Ray Studies of Liquid Crystal Transitions in Lipids. *Philos. Trans. R. Soc., A* **2006**, *364*, 2635–2655.
- (32) Israelachvili, J.; Mitchell, D.; Ninham, B. Theory of Self-Assembly of Hydrocarbon Amphiphiles into Micelles and Bilayers. *J. Chem. Soc., Faraday Trans. 2* **1976**, *72*, 1525–1568.
- (33) Israelachvili, J. N. *Intermolecular and Surface Forces*, 3rd ed.; Academic Press: London, 2011; p 674.
- (34) Dickey, A.; Faller, R. Examining the Contributions of Lipid Shape and Headgroup Charge on Bilayer Behavior. *Biophys. J.* **2008**, *95*, 2636–2646.
- (35) Venugopal, E.; Bhat, S. K.; Vallooran, J. J.; Mezzenga, R. Phase Behavior of Lipid-Based Lyotropic Liquid Crystals in Presence of Colloidal Nanoparticles. *Langmuir* **2011**, *27*, 9792–9800.
- (36) Angelov, B.; Angelova, A.; Papahadjopoulos-Sternberg, B.; Lesieur, S.; Sadoc, J.-F.; Ollivon, M.; Couvreur, P. Detailed Structure of Diamond-Type Lipid Cubic Nanoparticles. *J. Am. Chem. Soc.* **2006**, *128*, 5813–5817.
- (37) Angelov, B.; Angelova, A.; Garamus, V. M.; Drechsler, M.; Willumeit, R.; Mutafchieva, R.; Štěpánek, P.; Lesieur, S. Earliest Stage of the Tetrahedral Nanochannel Formation in Cubosome Particles from Unilamellar Nanovesicles. *Langmuir* **2012**, *28*, 16647–16655.
- (38) Quinn, P. J. A Lipid-Phase Separation Model of Low-Temperature Damage to Biological Membranes. *Cryobiology* **1985**, *22*, 128–146.
- (39) Voorhees, P. The Theory of Ostwald Ripening. *J. Stat. Phys.* **1985**, *38*, 231–252.
- (40) Chong, J. Y. T.; Mulet, X.; Waddington, L. J.; Boyd, B. J.; Drummond, C. J. Steric Stabilisation of Self-Assembled Cubic Lyotropic Liquid Crystalline Nanoparticles: High Throughput

Evaluation of Triblock Polyethylene Oxide-Polypropylene Oxide-Polyethylene Oxide Copolymers. *Soft Matter* **2011**, *7*, 4768–4777.

(41) Lenaerts, V.; Triqueneaux, C. Temperature-Dependent Rheological Behavior of Pluronic F-127 Aqueous Solutions. *Int. J. Pharm.* **1987**, *39*, 121–127.

(42) Bohorquez, M.; Koch, C.; Trygstad, T.; Pandit, N. A Study of the Temperature-Dependent Micellization of Pluronic F127. *J. Colloid Interface Sci.* **1999**, *216*, 34–40.

(43) Pandit, N.; Trygstad, T.; Croy, S.; Bohorquez, M.; Koch, C. Effect of Salts on the Micellization, Clouding, and Solubilization Behavior of Pluronic F127 Solutions. *J. Colloid Interface Sci.* **2000**, *222*, 213–220.

(44) Conn, C. E.; Darmanin, C.; Sagnella, S. M.; Mulet, X.; Greaves, T. L.; Varghese, J. N.; Drummond, C. J. Incorporation of the Dopamine D2L Receptor and Bacteriorhodopsin within Bicontinuous Cubic Lipid Phases. I. Relevance to in Meso Crystallization of Integral Membrane Proteins in Monoolein Systems. *Soft Matter* **2010**, *6*, 4828–4837.

(45) Lee, K. W. Y.; Nguyen, T.-H.; Hanley, T.; Boyd, B. J. Nanostructure of Liquid Crystalline Matrix Determines in Vitro Sustained Release and in Vivo Oral Absorption Kinetics for Hydrophilic Model Drugs. *Int. J. Pharm.* **2009**, *365*, 190–199.